

Non-universal gap structure in iron-based high- T_c superconductors

K. Hashimoto^{1,2,*}, M. Yamashita^{1,*}, S. Kasahara³, Y. Senshu¹, N. Nakata¹, S. Tonegawa¹, K. Ikada¹, A. Serafin², A. Carrington², T. Terashima³, H. Ikeda¹, T. Shibauchi¹, and Y. Matsuda¹

¹*Department of Physics, Kyoto University,
Sakyo-ku, Kyoto 606-8502, Japan*

²*H. H. Wills Physics Laboratory,*

University of Bristol, Tyndall Avenue, Bristol, UK

³*Research Center for Low Temperature and Materials Sciences,
Kyoto University, Sakyo-ku, Kyoto 606-8501, Japan*

**These authors contributed equally to this work.*

(Dated: July 9, 2009)

Experimental insight into the origin of the interactions which drive high temperature superconductivity can be gained from the anisotropy of the energy gap. In the high- T_c Fe-pnictide superconductors¹ most measurements to date indicate that the energy gap is finite at all points on the Fermi surface^{2,3,4,5,6,7}, in sharp contrast to high- T_c cuprates which have zeros (nodes) in the gap. Here we report magnetic penetration depth and thermal conductivity data for $\text{BaFe}_2(\text{As}_{1-x}\text{P}_x)_2$ ($T_c = 30$ K) which show unambiguously that this material has an energy gap with line nodes. This is distinctly different from the nodeless gap found for $(\text{Ba,K})\text{Fe}_2\text{As}_2$ which has similar T_c , electronic structure, and phase diagram. Our results indicate that repulsive electronic interactions play an essential role for Fe-based high- T_c superconductivity but that uniquely there are quasi degenerate pairing states, with and without nodes, which have similar T_c .

The most important question concerning the newly discovered Fe-based high temperature superconductors is what is the interaction that glues the electrons into Cooper pairs. Conventional phonon-mediated pairing leads to the superconducting gap opening all over the Fermi surface, while unconventional pairing mechanisms, such as spin fluctuations, lead to a gap which has opposite signs on some regions of the Fermi surface which is necessary to produce a net attractive pair-interaction in the presence of strong Coulomb repulsion between electrons. In high- T_c cuprate superconductors, where the electronic structure is essentially described by a single quasi-two-dimensional Fermi surface, the sign change of order parameter inevitably produces line nodes in the gap function. In Fe-pnictides, however, the Fermi surface has disconnected hole and electron sheets and so the condition for a sign changing gap can be fulfilled without nodes, leading to a distinct type of unconventional order parameter, known as an s_{\pm} state^{8,9}. In this case, each Fermi surface is fully gapped, preventing low-energy excitation of quasiparticles similar to conventional phonon-mediated superconductors.

Most experimental studies of high- T_c Fe-arsenides indicate a fully-gapped superconducting state^{1,2,3,4,5,6,7}. Although some measurements could be also consistent with nodes^{1,10}, the intrinsic behaviour may be obscured by disorder. The observation of an unusual resonance mode in neutron data¹¹ and the observation of half-integer flux jumps¹² point towards a sign changing gap consistent with an electronic pairing mechanism although an important role for phonons has also been established^{13,14}. Thus the nature of the high- T_c superconductivity in Fe-arsenides remains far from determined.

Recently, the isovalent substitution of P for As in

BaFe_2As_2 was found to induce superconductivity¹⁵ and high-quality single crystals with T_c as high as 31 K become available¹⁶. The substitution in the pnictogen site is expected to induce less scattering in the Fe-conducting plane than the substitution for Fe as in the case of $\text{Ba}(\text{Fe},\text{Co})_2\text{As}_2$ ($T_c \lesssim 24$ K). This nominally undoped system bears marked similarities to the hole doped $(\text{Ba,K})\text{Fe}_2\text{As}_2$ system. They have similar phase diagrams^{16,17}: their parent compound is the same (Fig. 1a) which has an antiferromagnetic spin-density-wave (SDW) ground state and high- T_c superconductivity with comparable maximum T_c appears in proximity to the SDW phase (Fig. 1b). In addition, as demonstrated in Figs. 1c-e, they possess similar electronic structures. Moreover, in both systems, the presence of the strong antiferromagnetic fluctuations associated with the neighbouring SDW phase has been found by NMR (Ref. 7 and K. Ishida (private communication)). Therefore a comparison of the gap structure in $\text{BaFe}_2(\text{As}_{1-x}\text{P}_x)_2$ and $(\text{Ba,K})\text{Fe}_2\text{As}_2$ is of crucial importance to get insight into the pairing mechanism of high- T_c superconductivity in Fe-pnictides.

Among others, low-temperature measurements of the magnetic penetration depth λ and thermal conductivity κ are particularly suitable probes of the gap structure of superconductors. λ is directly related to the superfluid density $n_s \propto \lambda^{-2}$, whose temperature dependence is directly determined by the gap function. κ probes low-energy quasiparticle excitations that carry entropy and the low-temperature thermal conductivity is governed by delocalized quasiparticles, which extend over the whole crystal; it is not contaminated by the localized states or nuclear contributions that may produce the Schottky anomaly in the specific heat. Both measure-

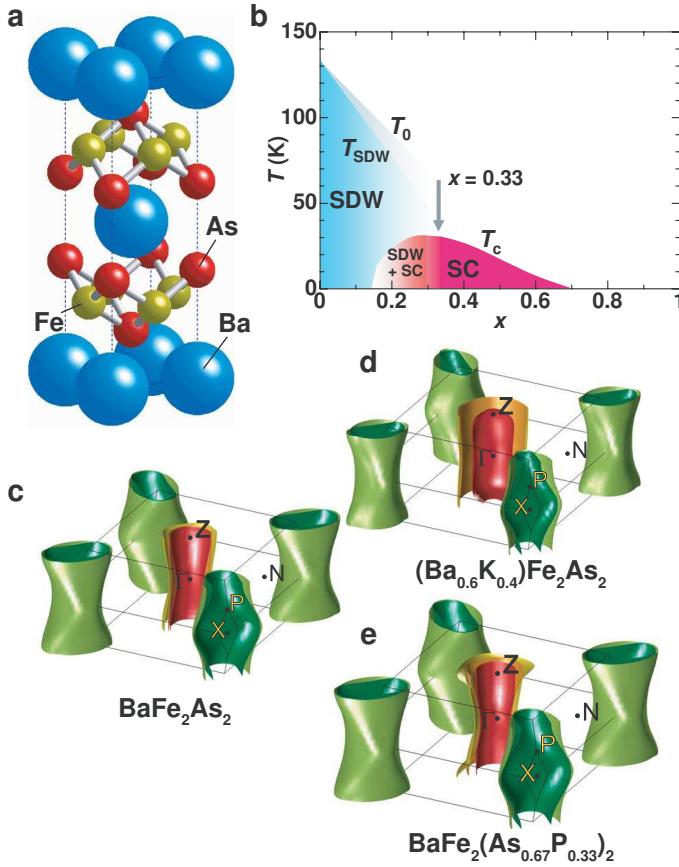


Figure 1: **The pnictogen-substitution system $\text{BaFe}_2(\text{As}_{1-x}\text{P}_x)_2$.** **a**, Schematic crystal structure of the parent compound BaFe_2As_2 . **b**, Phase diagram of temperature T versus P concentration x in $\text{BaFe}_2(\text{As}_{1-x}\text{P}_x)_2$ single crystals¹⁶. **c,d,e**, Fermi surfaces of BaFe_2As_2 (**c**), $\text{BaFe}_2(\text{As}_{0.67}\text{P}_{0.33})_2$ (**d**), and $(\text{Ba}_{0.6}\text{K}_{0.4})\text{Fe}_2\text{As}_2$ (**e**) obtained by band calculations using the density functional theory (see Supplementary Information).

ments probe the bulk superconducting properties and are not influenced by the surface electronic reconstructions which seem to be relevant to surface-sensitive probes in Fe-pnictides^{18,19}. Our $\text{BaFe}_2(\text{As}_{0.67}\text{P}_{0.33})_2$ crystals exhibit excellent bulk superconducting properties including a very sharp superconducting transition at $T_c = 30$ K (Fig. 2).

Figure 3a shows the normalized change in the penetration depth $\Delta\lambda(T)/\lambda(0)$ in $\text{BaFe}_2(\text{As}_{0.67}\text{P}_{0.33})_2$, compared with the reported results of a clean $(\text{Ba}_{0.45}\text{K}_{0.55})\text{Fe}_2\text{As}_2$ crystal⁵. In sharp contrast to the flat behaviour observed in the K-doped crystal, $\Delta\lambda(T)$ in the P-substituted crystal exhibits a strong quasi-linear temperature dependence at low temperatures. The T -linear dependence of $\Delta\lambda(T)$ is a strong indication of line nodes in the superconducting gap, and is similar to that reported in $\text{YBa}_2\text{Cu}_3\text{O}_{7-\delta}$ which has d -wave symmetry²⁰. The normalized superfluid den-

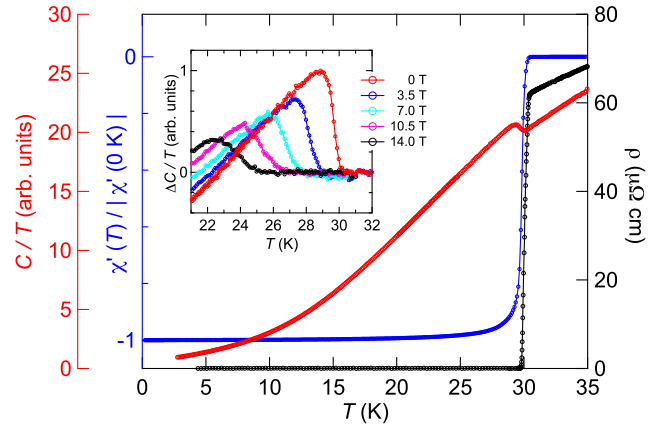


Figure 2: **Superconducting properties in single crystals of $\text{BaFe}_2(\text{As}_{0.67}\text{P}_{0.33})_2$.** Temperature dependence of the specific heat divided by temperature $C(T)/T$ (red curve) and the real part of rf susceptibility χ' (blue) in a single crystal sample. Typical temperature dependence of the in-plane resistivity $\rho(T)$ (black, right axis) of a crystal from the same batch is also shown. Inset shows an expanded view near T_c of the change $\Delta C(T)/T$ with the normal state contribution subtracted at several magnetic fields along the c axis.

sity $\lambda^2(0)/\lambda^2(T)$ in Fig. 3b also clearly demonstrates the fundamental difference between $\text{BaFe}_2(\text{As}_{0.67}\text{P}_{0.33})_2$ and $(\text{Ba}_{0.45}\text{K}_{0.55})\text{Fe}_2\text{As}_2$. The low-temperature data of $\text{BaFe}_2(\text{As}_{0.67}\text{P}_{0.33})_2$ can be fitted to $1 - \alpha(T/T_c)^n$ with the exponent $n = 1.1$, close to unity. This is completely incompatible with the flat exponential dependence observed in the fully gapped superconductors, and immediately indicates the low-lying quasiparticle excitations in this system. In the fully gapped unconventional s_{\pm} state, it has been suggested that the substantial impurity scattering may induce the in-gap states that alter the exponential superfluid density to the power-law dependence, but the exponent is expected to be not smaller than 2 (Refs. 21,22). Indeed, in some Fe-pnictides with larger scattering such as $\text{Ba}(\text{Fe},\text{Co})_2\text{As}_2$, the power-law dependence of superfluid density with powers varying $n \sim 2.0$ to ~ 2.4 has been reported^{5,10}. However, the present results with exponent significantly smaller than 2 and much closer to 1 expected for clean superconductors with line nodes, cannot be explained by these modifications of a full-gap state, but is indicative of well-developed line nodes in the gap.

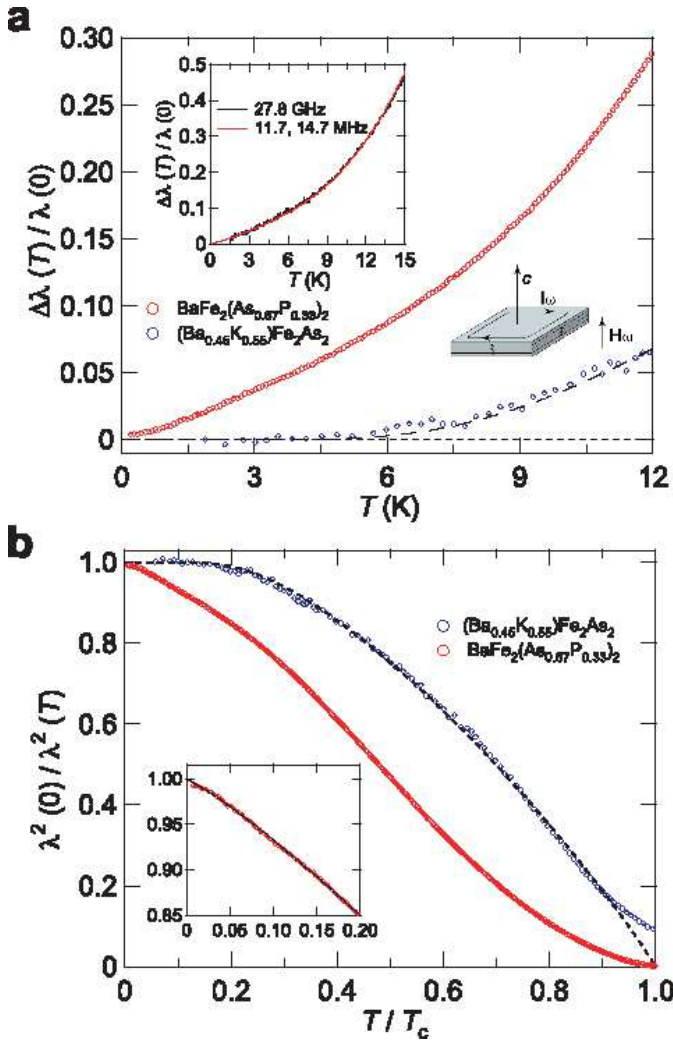


Figure 3: **Magnetic penetration depth in $\text{BaFe}_2(\text{As}_{0.67}\text{P}_{0.33})_2$.** **a**, The change $\Delta\lambda(T) \equiv \lambda(T) - \lambda(0)$ in the penetration depth in $\text{BaFe}_2(\text{As}_{0.67}\text{P}_{0.33})_2$ measured by the rf tunnel-diode oscillator. The vertical axis is normalized by the zero-temperature value $\lambda(0) = 200$ nm, which is obtained from the microwave surface impedance measurements. As shown in the inset, microwave measurements at 27.8 GHz down to 1.7 K and rf measurements at 11.7 MHz in a ^4He fridge and at 14.7 MHz in a dilution fridge down to 200 mK show an excellent agreement. In both measurements, an ac weak magnetic field is applied along the c axis, generating supercurrent in the ab plane as sketched. For comparison, also shown are the microwave results of $(\text{Ba}_{0.45}\text{K}_{0.55})\text{Fe}_2\text{As}_2$ ($T_c \simeq 33$ K) with the fit to a nodeless order parameter reported in Ref. 5. **b**, Normalized superfluid density $\lambda^2(0)/\lambda^2(T)$ is plotted as a function of normalized temperature T/T_c . The tail near T_c in $(\text{Ba}_{0.45}\text{K}_{0.55})\text{Fe}_2\text{As}_2$ is due to the skin depth effect at microwave frequencies⁵. Inset shows an expanded view at low temperatures with a fit (solid line) to the power-law dependence with the exponent 1.1 (see Supplementary Information).

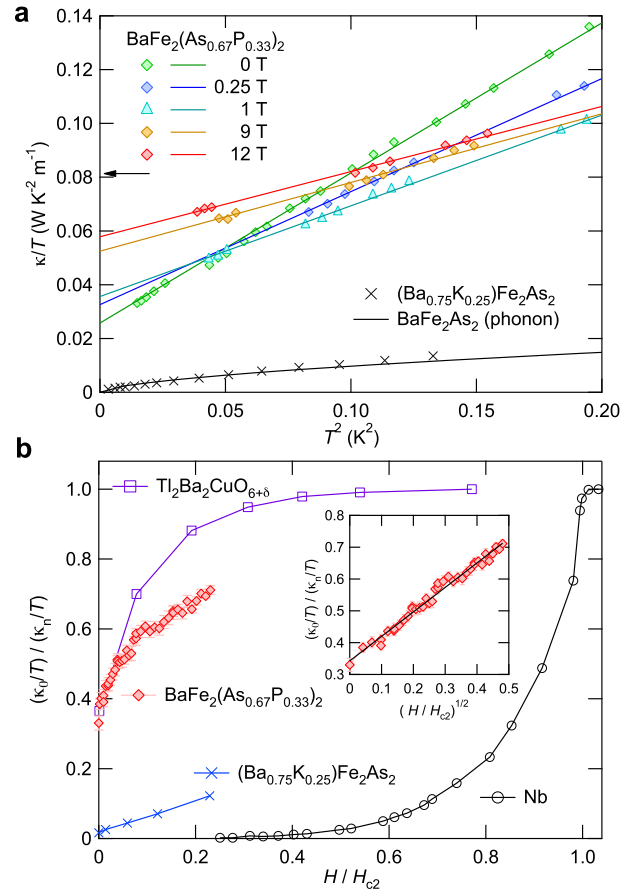


Figure 4: **Low-temperature thermal conductivity in $\text{BaFe}_2(\text{As}_{0.67}\text{P}_{0.33})_2$.** **a**, Thermal conductivity divided by temperature κ/T is plotted against T^2 measured under several magnetic fields applied along the c axis. The thermal current is applied in the ab plane. The lines are the best fits to $\kappa_0(H)/T + \beta(H)T^2$. The arrow indicates the normal-state value κ_n/T estimated from the Wiedemann-Franz law by using the residual resistivity ρ_0 which is obtained by the extrapolation of normal-state resistivity above T_c by assuming $\rho(T) = \rho_0 + AT$. For comparison, the reported data of $(\text{Ba}_{0.75}\text{K}_{0.25})\text{Fe}_2\text{As}_2$ ($T_c \simeq 30$ K)⁶ and the non-superconducting parent compound BaFe_2As_2 (Ref. 23) are also shown. The slope β in $\text{BaFe}_2(\text{As}_{0.67}\text{P}_{0.33})_2$ is much steeper than phonon contribution in BaFe_2As_2 , and decreases systematically with H consistent with the dominant quasiparticle contribution scattered by vortices (see Eq. 1). **b**, Residual $\kappa_0(H)/T$ for $\text{BaFe}_2(\text{As}_{0.67}\text{P}_{0.33})_2$ obtained by the extrapolation to $T \rightarrow 0$ K at each field value is plotted as a function of H/H_{c2} . Here the upper critical field $H_{c2} \approx 52$ T at $T = 0$ K is estimated from the initial slope of $H_{c2}(T)$ near T_c determined by the specific heat (see Supplementary Information). Also shown are the results for the cuprate superconductor $\text{Tl}_2\text{Ba}_2\text{CuO}_{6+\delta}$ with line nodes in the gap²⁵, and fully gapped superconductors Nb (Ref. 26) and $(\text{Ba}_{0.75}\text{K}_{0.25})\text{Fe}_2\text{As}_2$ (Ref. 6). The lines are guides for the eyes. In contrast to the P-substituted one, $\kappa(H)/T$ of K-doped one increases gradually with H , which has been attributed to the slight modulation of the gap value⁶. Inset shows the same data in $\text{BaFe}_2(\text{As}_{0.67}\text{P}_{0.33})_2$ plotted against $(H/H_{c2})^{1/2}$. The line is the best fit to the \sqrt{H} dependence expected for line nodes.

The thermal conductivity also provides a stringent test for the line nodes. First we address the temperature dependence of κ/T in zero field. In K-doped crystals $(\text{Ba}_{0.75}\text{K}_{0.25})\text{Fe}_2\text{As}_2$ ($T_c = 30$ K)⁶, $\kappa(T)/T$ is nearly identical to the phonon contribution κ_{ph}/T obtained from non-superconducting BaFe_2As_2 (Ref. 23), consistent with the fully-gapped superconductivity, in which very few quasiparticles are excited well below T_c (Fig. 4a). What is remarkable is that in spite of similar values of residual resistivity in the normal state^{6,16}, the magnitude of κ/T in $\text{BaFe}_2(\text{As}_{0.67}\text{P}_{0.33})_2$ is strikingly enhanced from that in $(\text{Ba}_{0.75}\text{K}_{0.25})\text{Fe}_2\text{As}_2$. Particularly, the presence of a residual value in κ_0/T ($\simeq 25$ W/K²m) at $T \rightarrow 0$ K is clearly resolved in $\text{BaFe}_2(\text{As}_{0.67}\text{P}_{0.33})_2$, while such a residual value is not discernible in $(\text{Ba}_{0.75}\text{K}_{0.25})\text{Fe}_2\text{As}_2$. In fact, it has been shown²⁴ that the quasiparticle thermal conductivity in superconductors with line nodes is given by

$$\frac{\kappa}{T} = \frac{\kappa_0}{T} \left(1 + O \left[\frac{T^2}{\gamma_0^2} \right] \right) \quad (1)$$

in the range $k_B T < \gamma_0$, where γ_0 is the impurity bandwidth. The term κ_0/T arises from the residual quasiparticles induced by the impurity scattering, no matter how small it is, in the presence of sign change of the order parameter. For line nodes, a rough estimation gives $\kappa_0/T \approx 22$ mW/K²m (see Supplementary Information), which reasonably coincides with the observed value. The second T^2 -term in Eq. (1) arises from the thermally excited quasiparticles around the nodes, which is also consistent with the observed quadratic temperature dependence of κ/T with a slope one order of magnitude larger than κ_{ph}/T .

Next we discuss the field dependence of κ_0/T , another independent test of the gap structure. The most distinguished feature in Fig. 4b is that $\kappa_0(H)/T$ increases steeply at low fields and attains nearly 70% of the normal-state value even at $0.2H_{c2}$. Such a field dependence is quite similar to that in $\text{Tl}_2\text{Ba}_2\text{CuO}_{6+\delta}$ with line nodes²⁵ but is in dramatic contrast to that in fully gapped superconductors such as Nb (Ref. 26). In fully gapped superconductors, quasiparticles excited by vortices are localized and unable to transport heat until these vortices are overlapped each other. In sharp contrast, the heat trans-

port in superconductors with nodes is dominated by contributions from delocalized quasiparticles outside vortex cores. The most remarkable effect on thermal transport is the Doppler shift of the quasiparticle energy. In the presence of line nodes where the density of states has a linear energy dependence $N(E) \propto |E|$, $N(H)$ increases steeply in proportion to \sqrt{H} . This is consistent with the field dependence of $\kappa_0(H)/T$ in $\text{BaFe}_2(\text{As}_{0.67}\text{P}_{0.33})_2$ shown in the inset of Fig. 4b. Thus, the presence of κ_0/T at zero field, the T^2 dependence of κ/T and the \sqrt{H} field dependence all lead us to conclude the presence of line nodes in the gap function of $\text{BaFe}_2(\text{As}_{0.67}\text{P}_{0.33})_2$, which provide a strong support on the results of the penetration depth.

The present results clearly indicate that line nodes exist in the gap function of $\text{BaFe}_2(\text{As}_{0.67}\text{P}_{0.33})_2$. An important question is then to answer how distinctly different gap structures (with and without nodes) can exist in very similar systems *and have comparable transition temperatures*. Although the Fermi surface topology is similar in these two systems (Figs. 1c-d), differences in the size and corrugation of hole surfaces may give rise to the dramatic change of the nodal topology. One possibility is that both systems have a *nodal s-wave* gap function but that the nodes are lifted by disorder²⁷ in the K-doped system. However, as these samples have almost identical T_c values and normal-state residual resistivities^{6,16} as well as similar enhancements in the microwave conductivity below T_c (S. Tonegawa *et al.*, unpublished results), this suggests that they have similar levels of disorder and so this scenario is unlikely. It has been pointed out that the pnictogen height sensitively changes the orbital character of one of the hole sheets, which may be the origin of the different pairing states⁹. This is consistent with the observation of a nodal pairing state in the iron-phosphide superconductor LaFePO (Refs. 28,29,30). However the nodal gap function generally leads to a much lower T_c (as in LaFePO where $T_c \sim 7$ K) so the high T_c of $\text{BaFe}_2(\text{As}_{1-x}\text{P}_x)_2$ remains puzzling. In any case, our results point to the presence of at least two pairing channels which have nearly degenerate energies. We believe this will help to uncover the mechanism of high- T_c superconducting in these materials.

¹ Ishida, K., Nakai, Y. & Hosono, H. To what extent iron-pnictide new superconductors have been clarified: A progress report. *J. Phys. Soc. Jpn.* **78**, 062001 (2009).

² Hashimoto K. *et al.* Microwave penetration depth and quasiparticle conductivity of PrFeAsO_{1-y} single crystals: Evidence for a full-gap superconductor. *Phys. Rev. Lett.* **102**, 017002 (2009).

³ Malone L. *et al.* Magnetic penetration depth of single-crystalline $\text{SmFeAsO}_{1-x}\text{F}_y$. *Phys. Rev. B* **79**, 140501(R) (2009).

⁴ Ding, H. *et al.* Observation of Fermi-surface-dependent nodeless superconducting gaps in $\text{Ba}_{0.6}\text{K}_{0.4}\text{Fe}_2\text{As}_2$. *Europhys. Lett.* **83**, 47001 (2008).

⁵ Hashimoto K. *et al.* Microwave surface-impedance measurements of the magnetic penetration depth in single crystal $\text{Ba}_{1-x}\text{K}_x\text{Fe}_2\text{As}_2$ superconductors: Evidence for a disorder-dependent superfluid density. *Phys. Rev. Lett.* **102**, 207001 (2009).

⁶ Luo, X.G. *et al.* Quasiparticle heat transport in $\text{Ba}_{1-x}\text{K}_x\text{Fe}_2\text{As}_2$: Evidence for a k -dependent su-

- perconducting gap without nodes. Preprint at (<http://arxiv.org/abs/0904.4049>) (2009).
- 7 Yashima, M. *et al.* Strong-coupling spin-singlet superconductivity with multiple full gaps in hole-doped $\text{Ba}_{0.6}\text{K}_{0.4}\text{Fe}_2\text{As}_2$ probed by ^{57}Fe -NMR. Preprint at (<http://arxiv.org/abs/0905.1896>) (2009).
 - 8 Mazin, I. I., Singh, D. J., Johannes, M. D. & Du, M. H. Unconventional superconductivity with a sign reversal in the order parameter of $\text{LaFeAsO}_{1-x}\text{F}_x$. *Phys. Rev. Lett.* **101**, 057003 (2008).
 - 9 Kuroki, K., Usui, H., Onari, S., Arita, R. & Aoki, H. Pnictogen height as a possible switch between high- T_c nodeless and low- T_c nodal pairings in the iron based superconductors. *Phys. Rev. B* **79**, 224511 (2009).
 - 10 Gordon, R. T. *et al.* The London penetration depth in single crystals of $\text{Ba}(\text{Fe}_{1-x}\text{Co}_x)_2\text{As}_2$ at various doping levels. *Phys. Rev. B* **79**, 100506(R) (2009).
 - 11 Christianson, A. D. *et al.* Unconventional superconductivity in $\text{Ba}_{0.6}\text{K}_{0.4}\text{Fe}_2\text{As}_2$ from inelastic neutron scattering. *Nature* **456**, 930–932 (2008).
 - 12 Chen, C.-T., Tsuei, C. C., Ketchen, M. B., Ren, Z.-A. & Zhao, Z. X. Integer and half-integer flux-quantum transitions in a niobium/iron-pnictide loop. Preprint at (<http://arxiv.org/abs/0905.3571>) (2009).
 - 13 Liu, R. H. *et al.* A large iron isotope effect in $\text{SmFeAsO}_{1-x}\text{F}_x$ and $\text{Ba}_{1-x}\text{K}_x\text{Fe}_2\text{As}_2$. *Nature* **459**, 64–67 (2009).
 - 14 Yildirim, T. Frustrated magnetic interactions, giant magneto-elastic coupling, and magnetic phonons in iron-pnictides. *Physica C* **469**, 425–441 (2009).
 - 15 Jiang, S. *et al.* Superconductivity in $\text{BaFe}_2(\text{As}_{1-x}\text{P}_x)_2$. Preprint at (<http://arxiv.org/abs/0901.3227>) (2009).
 - 16 Kasahara, S. *et al.* Evolution from non-Fermi to Fermi liquid transport properties by isovalent doping in $\text{BaFe}_2(\text{As}_{1-x}\text{P}_x)_2$ superconductors. Preprint at (<http://arxiv.org/abs/0905.4427>) (2009).
 - 17 Luo, H. *et al.* Growth and characterization of $\text{A}_{1-x}\text{K}_x\text{Fe}_2\text{As}_2$ ($\text{A} = \text{Ba}, \text{Sr}$) single crystals with $x = 0 - 0.4$. *Supercond. Sci. Technol.* **21** 125014 (2008).
 - 18 Lu, D. H. *et al.* Electronic structure of the iron-based superconductor LaOFeP . *Nature* **455**, 81–84 (2008).
 - 19 Niestemski, F. C. *et al.* Unveiling the atomic and electronic structure at the surface of the parent pnictide SrFe_2As_2 . Preprint at (<http://arxiv.org/abs/0906.2761>) (2009).
 - 20 Hardy, W. N., Bonn, D. A., Morgan, D. C., Liang, R. & Zhang K. Precision measurements of the temperature dependence of λ in $\text{YBa}_2\text{Cu}_3\text{O}_{6.95}$: Strong evidence for nodes in the gap function. *Phys. Rev. Lett.* **70**, 3999–4002 (1993).
 - 21 Vorontsov, A. B., Vavilov, M. G. & Chubukov, A. V. Superfluid density and penetration depth in Fe-pnictides. *Phys. Rev. B* **79**, 140507(R) (2009).
 - 22 Bang, Y. Superfluid density of the $\pm s$ -wave state for the iron-based superconductors. *Europhys. Lett.* **86**, 47001 (2009).
 - 23 Kurita, N. *et al.* Low-temperature thermal conductivity of BaFe_2As_2 : Parent compound of iron-arsenide superconductors. *Phys. Rev. B* **79**, 214439 (2009).
 - 24 Graf, M. J., Yip, S.-K., Sauls, J. A. & Rainer, D. Electronic thermal conductivity and the Wiedemann-Franz law for unconventional superconductors. *Phys. Rev. B* **53**, 15147–15161 (1996).
 - 25 Proust, C., Boaknin, E., Hill, R. W., Taillefer, L. & Mackenzie, A. P. Heat transport in a strongly overdoped cuprate: Fermi liquid and pure d -wave BCS superconductor. *Phys. Rev. Lett.* **89** 147003 (2002).
 - 26 Lowell, J. & Sousa, J. B. Mixed-state thermal conductivity of type II superconductors. *J. Low Temp. Phys.* **3**, 65–87 (1970).
 - 27 Mishra, V. *et al.* Lifting of nodes by disorder in extended- s state superconductors: Application to ferropnictides. *Phys. Rev. B* **79**, 094512 (2009).
 - 28 Fletcher, J. D. *et al.* Evidence for a nodal-line superconducting state in LaFePO . *Phys. Rev. Lett.* **102**, 147001 (2009).
 - 29 Hicks, C. W. *et al.* Evidence for nodal superconductivity in LaFePO from scanning SQUID susceptometry. Preprint at (<http://arxiv.org/abs/0903.5260>) (2009).
 - 30 Yamashita, M. *et al.* Superconducting gap structure of LaFePO studied by thermal conductivity. Preprint at (<http://arxiv.org/abs/0906.0622>) (2009).

Acknowledgments We thank H. Takeya and K. Hirata for the early-stage collaboration on the crystal growth, and K. Ishida, H. Kontani and K. Kuroki for helpful discussion. This work is partially supported by KAKENHI, Grant-in-Aid for GCOE program “The Next Generation of Physics, Spun from Universality and Emergence” from MEXT, Japan, and EPSRC in the UK.

Additional Information Correspondence and requests for materials should be addressed to T. S. (shibauchi@scphys.kyoto-u.ac.jp) or Y. M. (matsuda@scphys.kyoto-u.ac.jp).

Supplementary Information

I. CRYSTAL GROWTH AND CHARACTERIZATION

Single crystals of $\text{BaFe}_2(\text{As}_{1-x}\text{P}_x)_2$ were grown^{S1} from a mixture of FeAs, Fe, P (powders) and Ba (flakes). The mixture was placed in an alumina crucible and sealed in an evacuated quartz tube. To avoid explosion due to high vapour pressures, the quartz tube was sealed inside a outer stainless tube by arc-melting. The whole assembly was heated up and typically kept at 1150 - 1200°C for 12 hours, and then cooled slowly down to 900°C at the rate of 1.5°C/hour. Platelet crystals as large as $1 \times 1 \times 0.06 \text{ mm}^3$ with shiny (001) surfaces were extracted. Structural analysis was performed by single-crystal X-ray diffractometry using a four-circle diffractometer (MXC^x, MacScience). The P concentration x was determined by an energy dispersive X-ray (EDX) analyzer (EDAX, Keyence). We find that changes in the lattice parameters a , c and the distance z_{Pn} between the pnictogen position and the Fe-plane are well described by Vegard's law. The crystals were carefully cleaved before measurement to avoid any issues with surface contamination.

The specific heat C was measured by a modulated temperature technique, using light as a heat source and a chromel-constantan thermocouple. To obtain the relative change in the electronic specific heat in the inset of Fig. 2, the normal-state C/T at 14 T was fitted to a low order polynomial (extrapolated to temperatures below T_c) and subtracted from the C/T data at each field.

II. EXPERIMENTAL TECHNIQUES

A. Penetration depth

Measurements of the temperature dependence of the magnetic penetration depth λ were performed at the University of Bristol with a high resolution radio frequency susceptometer based on a self-resonant tunnel diode circuit. Two different set-ups were used: one mounted on a pumped ^4He refrigerator (base temperature $\sim 1.5 \text{ K}$) had a resonant frequency of 11.7 MHz and the other mounted on a dilution refrigerator (base temperature $\sim 0.1 \text{ K}$) had a resonant frequency of 14.7 MHz (Ref. S2). The circuit operates with an extremely small probe field ($H_{ac} < 10 \text{ mOe}$) so that the sample is always in the Meissner state. Changes in the resonant frequency are directly proportional to changes in the magnetic penetration depth as the temperature of the sample is varied. The calibration factor is determined from the geometry of the sample, and the total perturbation to the resonant frequency due to the sample, found by withdrawing the sample from the coil at low temperature^{S3}. The sample is mounted on a sapphire rod, the other end of which is glued to a copper block on which a RuO₂ or Cernox thermometer is mounted. The sample and rod are placed inside a solenoid which forms part of the resonant tank circuit. The sapphire sample holder is of very high purity and has a very small paramagnetic background signal, which was subtracted.

Microwave surface impedance measurements by the cavity perturbation technique in Kyoto University^{S4,S5} were also used to determine the penetration depth λ . We used a su-

perconducting Pb cavity resonator operating at 27.8 GHz in the TE₀₁₁ mode with a high quality factor $Q \sim 10^6$. To measure the surface impedance of the small single crystal with high precision, the cavity resonator is immersed in superfluid ^4He at 1.6 K and its temperature is stabilized within $\pm 1 \text{ mK}$. The crystal was mounted on a sapphire hot finger and placed at the antinode of the microwave magnetic field \mathbf{H}_ω ($\parallel c$ axis) so that the shielding currents \mathbf{I}_ω are excited in the ab plane (see the sketch in Fig. 3). The inverse of quality factor $1/Q$ and the shift in the resonance frequency are proportional to the surface resistance R_s and the change in the surface reactance $\Delta X_s = X_s(T) - X_s(0)$ respectively. In the superconducting state, the surface reactance is proportional to the penetration depth $X_s = \mu_0\omega\lambda$, where ω is the microwave angular frequency. In the normal state, the relation $R_s(T) = X_s(T) = (\mu_0\omega\rho/2)^{1/2}$ holds for the skin depth regime, from which the $\lambda(T)/\lambda(0)$ can be extracted^{S4}. By comparing with the dc resistivity $\rho(T)$ and $X_s(T)$, we evaluate $\lambda(0) = 200 \pm 30 \text{ nm}$.

B. Thermal conductivity

Thermal conductivity κ was measured in Kyoto University by the standard four-wire steady-state method in a dilution refrigerator^{S6,S7}. The thermal current was applied in the ab -plane and magnetic field was applied parallel to the c axis. Four contacts were made to the sample using a spot-welding technique which gave low contact resistances less than 100 m Ω . The temperature dependence of the thermal conductivity was measured in both field-cooling (FC) and zero-field cooling (ZFC) conditions at several fields. We observed no discernible difference between FC and ZFC, indicating that field trapping related to vortex pinning is negligibly small in the present T - and H -ranges. Also, we found a symmetric field dependence for positive and negative fields in the zero-field cooling measurements, which gives a further support for the irrelevance of pinning effects in our data.

III. FERMI SURFACE TOPOLOGY

Our band-structure calculations were performed using an augmented plane wave plus local orbital method as implemented in the WIEN2K code^{S8}. Calculations were carried out for the paramagnetic state of pure BaFe_2As_2 (Fig. 1c), $(\text{Ba}_{0.6}\text{K}_{0.4})\text{Fe}_2\text{As}_2$ (Fig. 1d) and $\text{BaFe}_2(\text{As}_{0.67}\text{P}_{0.33})_2$ (Fig. 1e). The parameters are listed in Table S1.

Table S1: Crystallographic parameters used for the band-structure calculations.

Compound	Ref.	a (Å)	c (Å)	z_{As}
BaFe_2As_2	S9	3.9609	12.9763	0.35500
$(\text{Ba}_{0.6}\text{K}_{0.4})\text{Fe}_2\text{As}_2$	S10	3.9117	13.3523	0.35358
$\text{BaFe}_2(\text{As}_{0.67}\text{P}_{0.33})_2$	–	3.9261	12.8202	0.35190

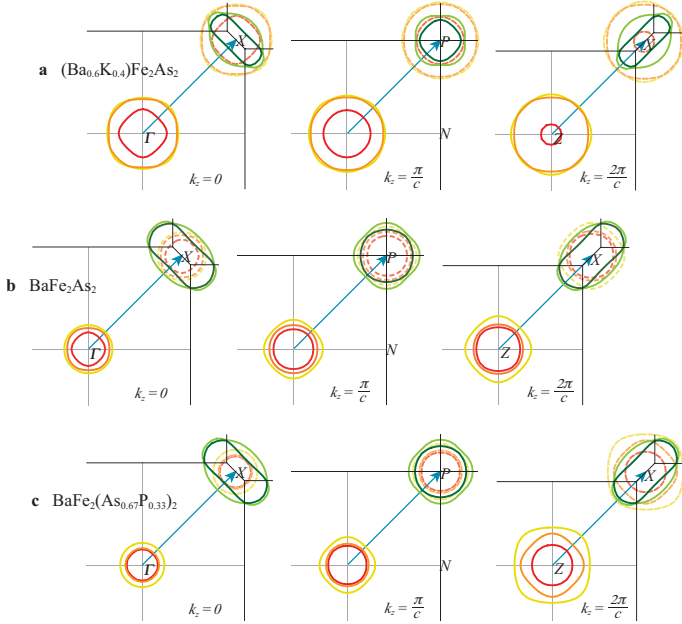


Figure S1: **The Fermi surfaces corresponding to $(\text{Ba}_{0.6}\text{K}_{0.4})\text{Fe}_2\text{As}_2$ (a), BaFe_2As_2 (b), and $\text{BaFe}_2(\text{As}_{0.67}\text{P}_{0.33})_2$ (c).** In order from left to right, the cross-sections at $k_z = 0$, π/c and $2\pi/c$. The sky-blue arrow represents the nesting vector $Q = (\pi/a, \pi/a, 0)$. Light dotted circles denote the hole surfaces shifted with Q .

For simplicity we have calculated electronic structure of the doped systems by changing just the lattice parameters and z_{As} from the parameters for the parent compound. For the K-doped case we have also adjusted the band filling using a rigid band shift. These assumptions should produce a reasonable guide to the changes with doping as it is known that the most important factors in determining the band structure are z_{As} and the c/a ratio^{S11,S12}.

In Fig. S1, we illustrate cross-sections of the Fermi surfaces in the (001) plane at the high-symmetry points. For all three cases the general topology of the Fermi surface is quite similar, with three hole cylinders around Γ and two electron cylinders around X . For the parent material (Fig. S1b) the electron and hole Fermi surfaces are close to nesting across much of the Fermi surface with $Q = (\pi/a, \pi/a, 0)$, (which corresponds to ordering vector in the SDW phase). Substituting either K or P leads to a decrease (to zero) of T_{SDW} . This is likely linked to a reduction of the area of Fermi surface which is close to fulfilling the nesting condition. This occurs in distinctly different ways for the two different substitutions. For the 33% P substituted material (Fig. S1c) the hole sheets are more corrugated making it more three dimensional (compare $k_z = 2\pi/c$ plane in Fig. S1b with that in Fig. S1c), and so surfaces are close to nesting only along restricted sections along the c^* axis. For the 40% K doped material the hole Fermi surfaces (Fig. S1a) become larger and the electron surfaces become smaller. The two largest hole cylinders now do not contribute to the nesting with Q . Thus, differences in the size and corrugation of the Fermi surface may be the key role in understanding the dramatic change of the nodal character in superconductivity shown in the present paper.

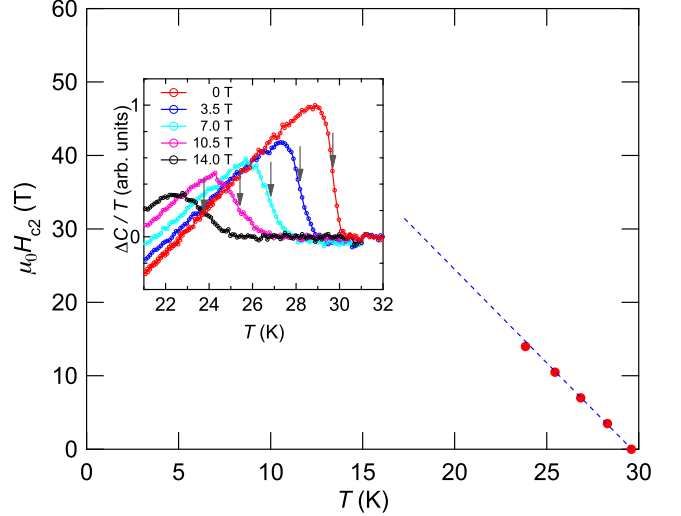


Figure S2: **Temperature dependence of the upper critical field $H_{c2}(T)$.** The dashed line gives the slope of dH_{c2}/dT near T_c . Inset shows specific heat data, from which we determine T_c by the mid point of the jump at each field (arrows).

IV. UPPER CRITICAL FIELD

The specific heat data shows a clear jump at T_c , which is used to determine the upper critical field $H_{c2}(T)$ in Fig. S2. The initial slope dH_{c2}/dT near T_c was found to be -2.56 T/K, from which we estimate $\mu_0 H_{c2}(0) = 52$ T by using the Werthamer-Helfand-Hohenberg (WHH) formula $H_{c2}(0) = -0.69T_c dH_{c2}/dT|_{T_c}$.

V. TEMPERATURE DEPENDENCE OF THE PENETRATION DEPTH

A. Exponent in the power law

In clean superconductors with line nodes, the normalized superfluid density $\lambda^2(0)/\lambda^2(T)$ exhibits a linear temperature dependence $1 - \alpha(T/T_c)^n$ with $n = 1$ for $T \ll T_c$ (the next term in the expansion is of order T^3). This gives $\Delta\lambda(T)/\lambda(0) = \frac{1}{2}\alpha(T/T_c) + \frac{3}{8}\alpha^2(T/T_c)^2 + \dots$ which leads to slightly concave (superlinear) temperature dependence for the penetration depth as we observed. Experimentally we obtain an exponent $n = 1.13(\pm 0.05)$ in a power law fit to the superfluid density assuming $\lambda(0) = 200$ nm. The uncertainty in $\lambda(0)$ is $\sim 15\%$ which leads to an uncertainty in n of $\sim 5\%$.

The fact that the experimental value of n is slightly larger than unity may result from impurity scattering. In the limit of high levels of disorder, a gap with line nodes gives $\Delta\lambda(T) \sim T^2$, and the following formula is often used to interpolate between the clean and dirty limits^{S13}, $\Delta\lambda(T) \propto T^2/(T + T^*)$. The disorder parameter T^* is related to the impurity band width γ_0 . If we use this formula to fit our data, we get $T^* \sim 1$ K, comparable to that of clean crystals of $\text{YBa}_2\text{Cu}_3\text{O}_{7-\delta}$

(Ref. S14). This suggests that our crystals are reasonably clean superconductors with line nodes.

B. Sample dependence

In Fig. S3, we compare the rf penetration depth measured in two samples of $\text{BaFe}_2(\text{As}_{0.67}\text{P}_{0.33})_2$ from the same batch. The overall temperature dependence is quite reproducible as can be seen in the main panel. At the lowest temperatures below ~ 0.5 K, we observe a small upturn whose magnitude is somewhat different between the two samples. We carefully checked, by measurements of a sample of the conventional superconductor Pb with similar dimensions, that this upturn is not due to artifacts from the background subtraction. The sample dependence of the upturn suggests that the most likely source of this is a small amount of paramagnetic impurities or residual flux.

Another possibility is that, as found in some crystals of high- T_c cuprate superconductors^{S15}, the surface Andreev bound states (ABS) are responsible for this anomaly. In cuprate superconductor the sign change of the order parameter leads to ABS at zero energy, which can enhance the penetration depth at very low temperatures on certain crystal faces. For the fully gapped s_{\pm} state, the sign change of the order parameter is predicted to lead to surface ABS at the sample edge in *finite* energies^{S16}. So whether this observation is related to the zero-energy ABS anomaly originating from the nodal structure found here deserves further studies. In any case, this effect is negligible for $T > 0.5$ K ($\sim 0.017T_c$), and is very small in sample #1, so this does not affect our conclusion of the existence of low-lying quasiparticle excitations in our system.

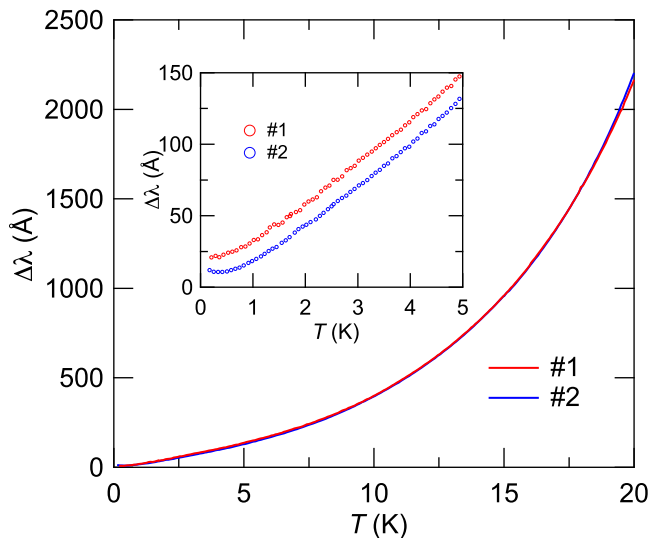


Figure S3: **Temperature dependence of the change in the penetration depth $\Delta\lambda(T)$ in two samples.** Inset shows an expanded view at low temperatures. The data for sample #1 (the same data as in Fig. 3 of the main paper) is shifted vertically for clarity.

VI. RESIDUAL κ_0/T IN SUPERCONDUCTORS WITH LINE NODES

For superconductivity with line nodes, the residual κ_0/T is described by $\frac{\kappa_0}{T} \simeq \frac{\kappa_n}{T} \frac{\hbar}{\tau} \frac{1}{\pi\Delta}$, where κ_n , τ and Δ are normal-state thermal conductivity, impurity scattering time and amplitude of the superconducting gap, respectively. By using the relation $\kappa_n/T = L_0/\rho_0$, κ_0/T is estimated to be $81 \text{ mW/K}^2\text{m}$, where L_0 is the Sommerfeld value $L_0 = 2.44 \times 10^{-8} \text{ } \Omega\text{W/K}$. ρ_0 is the residual resistivity which is obtained by the extrapolation of the resistivity above T_c by assuming $\rho(T) = \rho_0 + AT$. Using $\tau = \mu_0\lambda^2/\rho_0 = 1.7 \times 10^{-13} \text{ s}$ and $\Delta = 1.7k_B T_c$, κ_0/T is estimated to be $22 \text{ mW/K}^2\text{m}$. We note that with the parameters for $(\text{Ba}_{0.75}\text{K}_{0.25})\text{Fe}_2\text{As}_2$ Luo *et al.*^{S17} estimate $\kappa_0/T \approx 14 \text{ mW/K}^2\text{m}$, which is close to our estimate for $\text{BaFe}_2(\text{As}_{0.67}\text{P}_{0.33})_2$.

References

- S1. Kasahara, S. *et al.* Evolution from non-Fermi to Fermi liquid transport properties by isovalent doping in $\text{BaFe}_2(\text{As}_{1-x}\text{P}_x)_2$ superconductors. Preprint at (<http://arxiv.org/abs/0905.4427>) (2009).
- S2. Carrington, A., Giannetta, R.W., Kim, J.T. & Giapintzakis, J. Absence of nonlinear Meissner effect in $\text{YBa}_2\text{Cu}_3\text{O}_{6.95}$. *Phys. Rev. B* **59**, R14173–R14176 (1999).
- S3. Prozorov, R., Giannetta, R.W., Carrington, A. & Araujo-Moreira, F. M. Meissner-London state in superconductors of rectangular cross section in a perpendicular magnetic field. *Phys. Rev. B* **62**, 115–118 (2000).
- S4. Shibauchi, T. *et al.* Anisotropic penetration depth in $\text{La}_{2-x}\text{Sr}_x\text{CuO}_4$. *Phys. Rev. Lett.* **72**, 2263–2266 (1994).
- S5. Shimono, Y. *et al.* Effects of rattling phonons on the dynamics of quasiparticle excitation in the β -pyrochlore KOs_2O_6 superconductor. *Phys. Rev. Lett.* **98**, 257004 (2007).
- S6. Matsuda, Y., Izawa, K. & Vekhter I. Nodal structure of unconventional superconductors probed by the angle resolved thermal transport measurements. *J. Phys.: Condens. Matter* **18**, R705–R752 (2006).
- S7. Kasahara, Y. *et al.* Exotic superconducting properties in the electron-hole-compensated heavy-Fermion “Semimetal” URu_2Si_2 . *Phys. Rev. Lett.* **99**, 116402 (2007).
- S8. Blaha, P., Schwarz, K., Madsen, G.K.H., Kvasnicka, D. & Luitz, J. WIEN2K, An augmented plane wave + local orbitals program for calculating crystal properties (Karlheinz Schwarz, Techn. Universität Wien, Austria, 2001).
- S9. Gordon, R. T., *et al.* Unconventional London penetration depth in single-crystal $\text{Ba}(\text{Fe}_{0.93}\text{Co}_{0.07})_2\text{As}_2$ superconductors. *Phys. Rev. Lett.* **102**, 127004 (2009).
- S10. The lattice parameters were linearly extrapolated from the x dependence for $(\text{Ba}_{1-x}\text{K}_x)\text{Fe}_2\text{As}_2$ in “Rotter, M. *et al.* Competition of magnetism and superconductivity in underdoped $(\text{Ba}_{1-x}\text{K}_x)\text{Fe}_2\text{As}_2$. *New J. Phys.* **11**, 025014 (2009)”, and z_{As} was obtained from the ideal

tetrahedral bond angle of As-Fe-As indicated in “Rotter, M. *et al.* Superconductivity and crystal structures of $(\text{Ba}_{1-x}\text{K}_x)\text{Fe}_2\text{As}_2$ ($x = 0 - 1$). *Angew. Chem. Int. Ed.* **47**, 7949 (2008)”.

- S11. Mazin, I., Johannes, M. D., Boeri, L., Koepnik, K., & Singh, D. J. Problems with reconciling density functional theory calculations with experiment in ferropnictides. *Phys. Rev. B* **78**, 085104 (2008).
- S12. Singh, D. J. & Du, M.-H. Density functional study of $\text{LaFeAsO}_{1-x}\text{F}_x$: A low carrier density superconductor near itinerant magnetism. *Phys. Rev. Lett.* **100**, 237003 (2008).
- S13. Hirschfeld, P. J. & Goldenfeld, N. Effect of strong scattering on the penetration depth of a d -wave superconductor. *Phys. Rev. B* **48**, 4219–4222 (1993).
- S14. See, for example, Prozorov, R. & Giannetta, R. W. Magnetic penetration depth in unconventional superconductors. *Supercond. Sci. Tech.* **19**, R41–R67 (2006).
- S15. Carrington, A. *et al.* Evidence for surface Andreev bound states in cuprate superconductors from penetration depth measurements. *Phys. Rev. Lett.* **86**, 1074–1077 (2001).
- S16. Ghaemi, P., Wang, F. & Vishwanath, A. Andreev bound states as a phase-sensitive probe of the pairing symmetry of the iron pnictide superconductors. *Phys. Rev. Lett.* **102**, 157002 (2009).
- S17. Luo, X. G. *et al.* Quasiparticle heat transport in $\text{Ba}_{1-x}\text{K}_x\text{Fe}_2\text{As}_2$: Evidence for a k -dependent superconducting gap without nodes. Preprint at (<http://arxiv.org/abs/0904.4049>) (2009).